Morphology of crystalline surfaces under various step interaction potentials

2004 J. Phys.: Condens. Matter 16 1361

(http://iopscience.iop.org/0953-8984/16/8/019)

INSTITUTE OF PHYSICS PUBLISHING JOURNAL OF PHYSICS: CONDENSED MATTER

J. Phys.: Condens. Matter **16** (2004) 1361–1374 PII: S0953-8984(04)69990-5

Morphology of crystalline surfaces under various step interaction potentials

Metin Ozdemir

Department of Physics, Cukurova University, 01330 Adana, Turkey

E-mail: metoz@cu.edu.tr

Received 6 October 2003
Published 13 February 2004
Online at stacks.iop.org/JPhysCM/16/1361 (DOI: 10.1088/0953-8984/16/8/019)

Abstract

We study the morphological equilibration of a periodically corrugated one-dimensional crystalline surface under various forms of interaction between neighbouring atomic steps on the surface. The surface under consideration is assumed to be below its roughening temperature and only surface diffusion is considered as a means of mass transport. Both continuum and discrete equations of motion for surface evolution are derived and compared. Continuum equations and discrete equations of motion in the limit of 'diffusion limited growth' lead to the same form of the variation of the height of the surface. The discrete equations provide additional information on the evolution of crystal height and terrace separations in the limit of 'step attachment/detachment limited growth'. While the shape of the evolving surface is determined by the dominant type of step–step interaction between neighbouring steps on the surface, the time dependence of terrace widths and thus of the height of the crystal depends on the dominant surface process for a given type of the step–step interaction. The variation of height of the corrugation depends on time as t, e^{-t}, t^{-1}, $t^{-1/2}$ and $t^{-1/3}$ and the height variation scales with the period of the corrugation wavelength λ as λ^3, λ^4, λ^5 and λ^6 in connection with the type of interaction between steps and the dominant atomic processes on the surface.

1. Introduction

Morphological equilibration of periodic crystalline surfaces has been a subject of study for a long time [1]. When the surface under consideration is below its roughening temperature T_R [2], the surface mainly consists of monatomic steps separated by flat terraces. Since the two-dimensional periodic structure of the surface is interrupted at the step edges, many surface phenomena such as crystal growth, etching and equilibration occur through particle attachment/detachment at the step edges. As a result surface evolution occurs only through the motion of atomic steps on the surface and therefore step–step interactions become important,

which is the driving force for step movements. For a comprehensive understanding of the surface processes just mentioned it is necessary to have a detailed knowledge of step movement on the surfaces. One-dimensional periodic profiles are ideal structures for which to study the evolution of surfaces through the movement of steps. This is because they can be produced easily experimentally and the motion of parallel straight steps formed on these surfaces can be handled more appropriately theoretically.

This paper is concerned with the time dependence of the shape and height of one-dimensional periodically corrugated crystalline surfaces when mass transport occurs only by surface diffusion and when there is no particle flux to the surface from a third dimension. Below T_R, the surface tension (surface free energy) $\gamma(\hat{n})$ is a function of the surface orientation $\hat{n}$ and is not an analytic function. $\gamma(\hat{n})$ has cusps along particular orientations and facets form on the equilibrium surface corresponding to these directions. Surface tension projected along a particular direction can be expanded in terms of various orders of surface slope in the continuum limit or in terms of various orders of step separations in the discrete case, each of which represents a special form of step–step interaction. Using this expansion for surface tension, continuum equations of motion for surface evolution and discrete equations of motion for individual steps are derived for all forms of step–step interactions considered in this study and they are compared in various limiting surface processes. Surface evolution is considered in the 'diffusion limited' (DL) and 'step attachment/detachment limited' (SL) growth regimes separately. The treatment of the subject, in spirit, follows the same lines as that presented in [3]

The plan of the paper is as follows. In section 2 continuum equations for surface evolution are derived using Mullins' phenomenological equations for each term in the expansion of projected surface tension corresponding to a particular form of step–step interaction. Analytical solutions for the time dependence of the surface height are found for each type of interaction. No attempt is made to solve for the profile of the surface in this section. In section 3 discrete equations of motion for each step on the surface are derived and solved numerically for each type of interaction in the two limits of surface processes (DL and SL). Surface evolution and height variation are considered in the DL and SL limits for all cases. The scaling of the crystal height variation with wavelength is found from numerical simulations. Analytical solutions for the time evolution of terrace widths are also presented in both limits of surface processes just mentioned. Section 4 contains a summary of results and conclusions.

2. Continuum equations of motion

Let us consider a one-dimensional continuous periodic surface described by a function $z(x, t)$ as shown in figure 1. Surface tension $\gamma(\hat{n})$ is a non-analytic function of surface orientation $\hat{n}$ below the roughening temperature (T_R) of the surface under consideration. The projected surface tension defined as

$$G(z_x) = \gamma(z_x)(1 + z_x)^{1/2} \tag{1}$$

where $z_x = \partial z/\partial x$ is the slope of the surface can be expanded in a series as

$$\begin{aligned} G &= G_0 + G_1|z_x| + \tfrac{1}{2}G_2 z_x^2 + \tfrac{1}{3}G_3|z_x|^3 + \tfrac{1}{4}G_4 z_x^4 + \tfrac{1}{5}G_5|z_x|^5 + \cdots \\ &= G_0 + \sum_{n=1}^{5} \frac{1}{n} G_n |z_x|^n + \cdots \end{aligned} \tag{2}$$

where G_0 is the free energy of a flat surface (facet) and the second term represents the free energy of a step. The presence of a quadratic term in this expansion is a matter of debate [8, 9] but we will include it since our main purpose here is to consider the effect of each term in

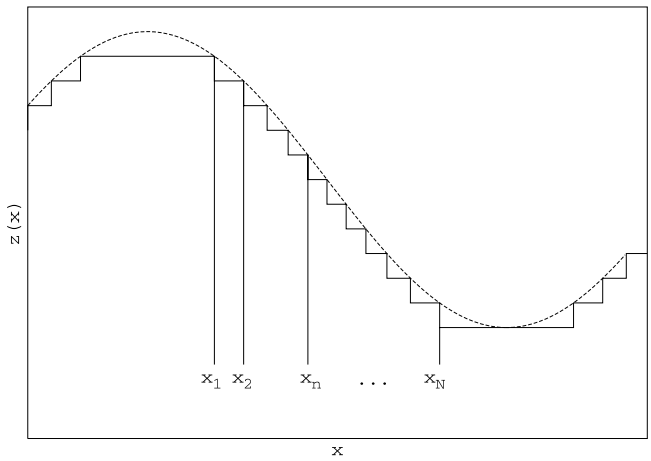

Figure 1. A typical geometry of the sample used in the simulations. The x_i are the time dependent positions of steps on the surface and the distance between two neighbouring steps is $\ell_i(t) = x_{i+1} - x_i$. The height of the surface goes down as a result of collisions and annihilations of steps at the top and the coalescence of steps at the bottom of the profile.

the expansion on the surface evolution separately and compare them. The remaining terms represent various forms of step–step interactions. The third order term represents step–step interactions which may result from elastic [4–6] or entropic [7] interactions. The fourth- and fifth-order terms originate from quadrupoles at the step interacting with force dipoles [10, 11].

When mass transport occurs by surface diffusion only, the time variation of the surface is given by

$$\frac{\partial z}{\partial t} = -\Omega \frac{\partial j}{\partial x} \tag{3}$$

where Ω is the volume of the diffusing particles on the surface and the surface current $j(x, t)$ is given by

$$j = -\frac{\nu D_s}{k_B T} \frac{\partial \mu}{\partial x} \tag{4}$$

where ν is the aerial density of particles participating in the diffusion process, D_s is the surface diffusion constant, k_B is Boltzmann's constant, T is the absolute temperature and $\mu(x, t)$ is the chemical potential of adsorbed species on the surface and is given by [12, 13]

$$\mu = -\Omega \frac{\partial}{\partial x}\left[\frac{\partial G}{\partial z_x}\right]. \tag{5}$$

We have assigned the conventional value $\nu = a^{-2}$ where a is the lattice constant. Both equations (3) and (4) are written with the small slope approximation in mind; otherwise the derivatives must be with respect to an arc length of the surface.

Now we will consider each of the terms in expansion (2), one by one, and obtain surface evolution equations using equations (3)–(5). Let us consider the term with coefficient G_2, namely the quadratic term in (2) first. This leads to the well known Mullins equation

$$\frac{\partial z}{\partial t} = -B_2 \frac{\partial^4 z}{\partial x^4} \tag{6}$$

where B_2 is given in equation (10) below and, if one assumes a separated solution of the form

$$z(x, t) = a(t)u(x) \tag{7}$$

to this equation, an arbitrary initial periodic profile of the form $u(x) = u_0 \sin(\frac{2\pi}{\lambda}x)$ with period λ decays exponentially and preserves its shape throughout its evolution as [13, 14]

$$z(x,t) = u_0 \sin\left(\frac{2\pi}{\lambda}x\right) \exp(-B_2(2\pi/\lambda)^4 t). \tag{8}$$

The evolution of the height scales as λ^4 with respect to the wavelength of the corrugation. When all terms in (2) are considered the equation of motion can be shown to be given by [3, 15]

$$\frac{\partial z}{\partial t} = -\sum_{\alpha=1}^{4} B_{\alpha+1} \frac{\partial^2}{\partial x^2}(|z_x|^{\alpha-1} z_{xx}) \tag{9}$$

where

$$B_{\alpha+1} = \frac{\alpha \Omega^2 D_s G_{\alpha+1}}{a^2 k_B T}, \qquad \alpha = 1, 2, 3, 4. \tag{10}$$

Let us now consider each of the terms in (9), one at a time. We have already considered the quadratic term. When only the third-order term with G_3 is considered the differential equation of surface evolution becomes

$$\frac{\partial z}{\partial t} = -B_3 \frac{\partial^2}{\partial x^2}(|z_x| z_{xx}) \tag{11}$$

and when a separated solution of the form given in (7) is assumed one obtains the equation

$$B_3 \frac{\partial^2}{\partial x^2}(|u_x| u_{xx}) = -k_3 u \tag{12}$$

for the space part and a solution of the form

$$a(t) = \frac{1}{k_3 t + 1} \tag{13}$$

where k_3 is a positive separation constant for the time dependence of the height of the corrugation as shown previously [3]. Similarly when the fourth- and fifth-order terms in (2) with coefficients G_4 and G_5 are considered separately the differential equations that give the time evolution of the surface become, respectively,

$$\frac{\partial z}{\partial t} = -B_4 \frac{\partial^2}{\partial x^2}(z_x^2 z_{xx}) \tag{14}$$

and

$$\frac{\partial z}{\partial t} = -B_5 \frac{\partial^2}{\partial x^2}(|z_x|^3 z_{xx}). \tag{15}$$

Again when a separated solution of the form (7) is assumed for these equations, the space dependent parts become, respectively,

$$B_4 \frac{\partial^2}{\partial x^2}(|u_x|^2 u_{xx}) = -k_4 u, \tag{16}$$

$$B_5 \frac{\partial^2}{\partial x^2}(|u_x|^3 u_{xx}) = -k_5 u \tag{17}$$

where k_4 and k_5 are positive separation constants and the solutions to the height function corresponding to equations (16) and (17) turn out to be

$$a(t) = \frac{1}{(2k_4 t + 1)^{1/2}} \tag{18}$$

and

$$a(t) = \frac{1}{(3k_5 t + 1)^{1/3}} \tag{19}$$

respectively. As can be seen, a variety of solutions exist for the time dependence of the height of the corrugation depending on the dominant form of step interactions. The general solution for the height function when all terms in (2) are considered will be very complicated and it will not be a linear combination of the functions given in (8), (13), (18) and (19) since the underlying differential equation is not linear. The time dependence of the height of the corrugation can be one of the functions just mentioned only when the corresponding interaction term is dominant among them. In a particular experiment the behaviour of the height evolution will be a result of all terms in (2). In the next section these results for the height evolution will be recovered once again when discrete equations of motion for each of the steps are derived and solved numerically in the DL growth regime. As we will see in the following section, additional time dependence behaviour not predicted by continuum equations results in the limit of the SL growth regime as well. We will make no attempt to solve the space dependent part of the equations, namely equations (12), (16) and (17), in this section.

3. Discrete equations of motion

In this section we derive an equation of motion for each step on the surface and solve them with a combination of analytical and numerical methods. From the motion of the steps, the morphology of the surface and the evolution of its height as a function of time are obtained. The results are compared with those of the previous section in the appropriate limits of surface processes. Let us consider a one-dimensional surface consisting of monatomic steps separated by terraces as shown in figure 1. The heights of the steps are taken to be equal to the lattice constant a. Noting that the slope of the surface can be written as $z_x = a/\ell$ where a is the height of a monatomic step and ℓ is the separation between neighbouring steps, we can rewrite equation (2) in terms of step separations as

$$G = G_0 + G_1|z_x| + \frac{1}{2}G_2\frac{a^2}{L}\sum\frac{1}{\ell_n} + \frac{1}{3}G_3\frac{a^3}{L}\sum\frac{1}{\ell_n^2} + \frac{1}{4}G_4\frac{a^4}{L}\sum\frac{1}{\ell_n^3} + \frac{1}{5}G_5\frac{a^5}{L}\sum\frac{1}{\ell_n^4} + \cdots \tag{20}$$

where $L = \sum \ell_n$ is half of the wavelength λ of the corrugation. When one considers half of the surface corrugation as is done here, then all steps will have the same sign. The interaction of steps with opposing signs, namely the steps at the top and bottom of the profile in figure 1, are neglected.

The motions of steps occur by the attachment/detachment of atoms to/from step edges. From the variation of the projected surface free energy (20) when a row of atoms is added/removed to/from the edge of a step by the atomistic processes just mentioned, one can define the 'chemical potential' of the nth step as [3, 16]

$$\mu_n = \sum_{\alpha=1}^{4} K_{\alpha+1}\left(\frac{1}{\ell_n^{\alpha+1}} - \frac{1}{\ell_{n-1}^{\alpha+1}}\right) \tag{21}$$

where

$$K_{\alpha+1} = \frac{\alpha}{\alpha+1}G_{\alpha+1}\frac{a^{\alpha+1}}{L}a^2, \qquad \alpha = 1, 2, 3, 4. \tag{22}$$

Slightly different equations are obtained for μ_n for the first ($n = 1$) and last ($n = N$) steps (see figure 1). The equation of motion of a step n can be written as [3]

$$\begin{aligned}\frac{\mathrm{d}x_n}{\mathrm{d}t} &= k_+[\Delta\bar{\mu}_n(x) - \mu_n]_+ + k_-[\Delta\bar{\mu}_{n-1}(x) - \mu_n]_- \\ &= v_n^+ + v_n^-\end{aligned} \tag{23}$$

where $\Delta\bar{\mu}_n(x)$ stands for the difference between the chemical potential $\bar{\mu}_n(x)$ of particles freely diffusing on the nth terrace and that of the constant chemical potential μ_c of an atom bound to the crystal at the step edge, μ_n is the chemical potential of the nth step just derived, and $k_\pm$ are the kinetic coefficients of the step. The $\pm$ signs standing just beneath the square brackets indicate that the relevant quantity to be evaluated is at a point just to the right (+) and to the left (−) of a step. v_n^+ is the velocity of the step due to the particle exchange with the terrace just in front of the step and similarly v_n^- is the velocity of the step due to particle exchange with the terrace just behind the step. An equation similar to (23) can be written from mass conservation as

$$\frac{\mathrm{d}x_n}{\mathrm{d}t} = \frac{D_s}{\nu}\left[\left.\frac{\mathrm{d}c_n(x)}{\mathrm{d}x}\right|_{x_n^+} - \left.\frac{\mathrm{d}c_{n-1}(x)}{\mathrm{d}x}\right|_{x_n^-}\right] = v_n^+ + v_n^- \tag{24}$$

where $c_n(x)$ is the concentration of diffusing particles on the nth terrace and is the solution of the steady state diffusion equation

$$\frac{\partial c_n(x)}{\partial t} = D_s\frac{\partial^2 c_n(x)}{\partial x^2} = 0 \tag{25}$$

given by

$$c_n(x) = a_n + b_n x, \qquad x_n \leqslant x \leqslant x_{n+1}. \tag{26}$$

Making appropriate expansions of the chemical potential difference $\Delta\bar{\mu}(x)$ in (23) and using equations (24) and (26) one can solve for the b_n in (26) as

$$b_n = \frac{\mu_{n+1} - \mu_n}{\left(\frac{\partial\bar{\mu}}{\partial c}\right)[d + \ell_n]} \tag{27}$$

where $d = a^2 D_s(k_+^{-1} + k_-^{-1})/(\partial\bar{\mu}/\partial c)$ is a quantity in units of length which measures the relative importance of surface diffusion on the terraces to the particle exchange rate at the step edges and $\ell_n = x_{n+1} - x_n$ is the distance between neighbouring steps. The equation of motion for a step labelled n can be written in terms of the b_n as

$$\frac{\mathrm{d}x_n}{\mathrm{d}t} = a^2 D_s(b_n - b_{n-1}) \tag{28}$$

which after some rearrangement becomes

$$\frac{\mathrm{d}x_n}{\mathrm{d}t} = \frac{(\mu_{n+1} - \mu_n)}{[d + \ell_n]} - \frac{(\mu_n - \mu_{n-1})}{[d + \ell_{n-1}]} \tag{29}$$

where the factor $a^2 D_s(\frac{\partial\bar{\mu}}{\partial c})^{-1}$ is absorbed in t.

We will now present analytical solutions for the time dependence of terrace widths in certain limits of surface processes when the surface possesses a particular profile. From equation (28) one can write the time dependence of the step separations $\ell_n(t)$ as

$$\dot{\ell}_n(t) = a^2 D_s(b_{n+1} - 2b_n + b_{n-1}). \tag{30}$$

The solutions of these equations when only one of the step interaction terms in (21) is considered ($\alpha = 1, 2, 3$ or 4) can be found by proposing an equation of the form

$$\ell_n(t) = A_n(gt + D)^\zeta \tag{31}$$

where g, D and the A_n are constants yet to be determined. The solutions turn out to be

$$\ell_n(t) = A_n[(\alpha + 3)\eta t + D]^{1/(\alpha+3)} \tag{32}$$

for the DL regime and

$$\ell_n(t) = A_n[(\alpha + 2)\eta t + D]^{1/(\alpha+2)} \tag{33}$$

for the SL regime where η is a positive separation constant and $\alpha = 1, 2, 3$ or 4. η is taken to be $(\alpha + 3)^{-1}$ in the DL regime and $(\alpha + 2)^{-1}$ in the SL regime throughout this paper. The A_n actually represent the space dependent part of the solution and they satisfy the equations

$$S_{n+1} - 2S_n + S_{n-1} = \eta A_n \tag{34}$$

where

$$S_n = \frac{1}{A_n}\left(\frac{1}{A_{n+1}^{\alpha+1}} - \frac{2}{A_n^{\alpha+1}} + \frac{1}{A_{n-1}^{\alpha+1}}\right) \tag{35}$$

for the DL regime and

$$S_n = \frac{1}{d}\left(\frac{1}{A_{n+1}^{\alpha+1}} - \frac{2}{A_n^{\alpha+1}} + \frac{1}{A_{n-1}^{\alpha+1}}\right) \tag{36}$$

for the SL regime. For both cases of DL and SL regimes, and for all values of α (=1, 2, 3 or 4) the initial profile must satisfy the condition

$$\frac{\ell_1(0)}{A_1} = \frac{\ell_2(0)}{A_2} = \cdots = \frac{\ell_N(0)}{A_N} \tag{37}$$

for the solutions (32) and (33) to be true. This assigns a particular shape to the profile and the solutions given in (32) and (33) are only valid when the number of steps N on the profile is constant and when the surface profile reaches the shape determined by equation (37). Any periodic profile far from (37) eventually reaches that shape preserving solution and remains so as long as there are no step annihilations at the top and there are no step coalescences at the bottom of the profile (figure 1).

To determine the shape preserving solution (37) the A_n must be known. These are solved from equations (34)–(36) using Newton's method generalized for multi-dimensional root finding [19] for each value of α. The S_n given in (35)–(36) are slightly different for the two steps at the top ($n = 1, 2$) and at the bottom ($n = N - 1, N$) of the profile and these actually form the boundary conditions needed for the solution of discrete equations (34). For a given type of step–step interaction, i.e. for a given value of α, the solutions for the A_n for the DL and SL regimes differ by nearly a constant. This means that the shape of the evolving surface is exclusively determined by the dominant type of step–step interactions. On the other hand, for a particular type of step–step interaction, the time dependence of the decay of the height of the corrugation is determined by the dominant atomic processes involved, namely by the DL or SL regime. Thus identical time dependence of the height of the crystal may result even if the dominant step interaction terms are different, as one can see from the summary of results shown in table 1. Therefore only if both the time dependence of the height of the crystal and the shape of the profile are known can both the dominant type of step–step interaction (if there is one) and the growth limiting surface process (DL or SL) be determined.

Numerical solutions for the A_n in the DL and SL regimes are shown in figures 2 and 3, respectively, on a logarithmic scale. The dependence of A_n on n for each type of step interaction for small n (steps that are close to the top of the profile) is shown in table 1. The exponents of n shown are found from the slopes of the best straight line fits (dashed lines) to the data points in figures 2 and 3 where only the first few data points are considered in the fits. The A_n represent the space dependent part of the solution as previously indicated. The top of the profile when only the quadratic term is considered is expected to obey $\delta z \approx (\delta x)^2$. This translates to $A_n \approx n^{-1/2}$ in terms of the dependence of A_n on n. Similarly the top of the profile must follow $(\delta x)^{3/2}$, $(\delta x)^{4/3}$ and $(\delta x)^{5/4}$, respectively, when the third-, fourth- and fifth-order terms are dominant in the surface free energy (2). These are expressed in terms of the A_n as $n^{-1/3}$, $n^{-1/4}$ and $n^{-1/5}$, in that order. To generalize these results, note that the top of the

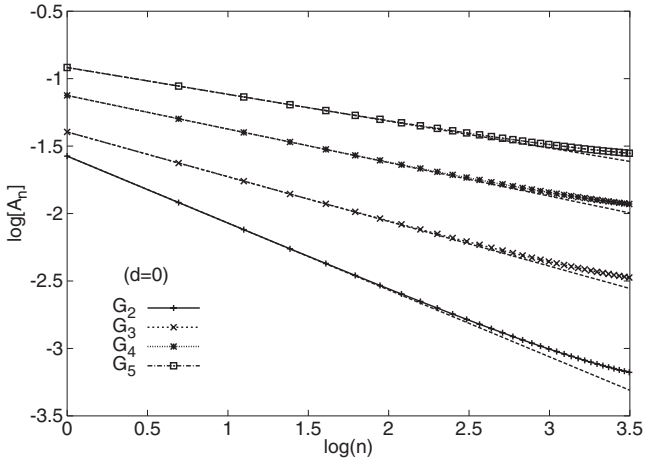

Figure 2. The variation of the A_n as a function of n on a log–log plot for each form of step–step interaction term in (2) in the diffusion limited (DL) growth regime. These are found from numerical solutions of equations (34). The variations for quadratic interactions are shown as plus signs. The straight dashed lines passing through these points are the best least squares straight line fits obtained taking only the first few data points. The slope of the straight line is $-1/2$ for quadratic interactions. Similar curves for third-, fourth- and fifth-order interaction terms are represented by crosses, filled circles with crosses and open squares, respectively. The slopes of the best straight line fits for these cases are, respectively, $-1/3$, $-1/4$ and $-1/5$.

Table 1. The decay of the surface profile with time, the scaling of the height of the profile with the wavelength λ and the variation of the A_n in equation (34) with respect to the type of interaction between steps in the two limiting (DL and SL) surface processes. The continuum equations and the discrete equations in the DL regime give identical time dependences of the height of the crystal surface (a and b are arbitrary constants). The scaling behaviours shown here are obtained from numerical solutions.

	DL ($d = 0$) regime			SL ($d = \infty$) regime			
Interaction	$h(t)$	$\ell_n(t)$	Scaling	$h(t)$	$\ell_n(t)$	Scaling	A_n
G_2	e^{-t}	$t^{1/4}$	λ^4	$a - bt$	$t^{1/3}$	λ^3	$n^{-1/2}$
G_3	t^{-1}	$t^{1/5}$	λ^5	e^{-t}	$t^{1/4}$	λ^4	$n^{-1/3}$
G_4	$t^{-1/2}$	$t^{1/6}$	λ^6	t^{-1}	$t^{1/5}$	λ^5	$n^{-1/4}$
G_5	$t^{-1/3}$	$t^{1/7}$	λ^7	$t^{-1/2}$	$t^{1/6}$	λ^6	$n^{-1/5}$

profile follows the dependence $\delta z \approx (\delta x)^{(\alpha+1)/\alpha}$ which corresponds to $A_n \approx n^{-1/(\alpha+1)}$ where $\alpha = 1, 2, 3$ or 4.

We will now present numerical solutions of equations (29) and the resulting surface morphologies, time dependences of terrace widths and crystal height as a function of time. The solutions are considered in the 'surface diffusion limited growth ($d \ll \ell_n$)' (DL) and 'step attachment/detachment limited growth ($d \gg \ell_n$)' (SL) regimes separately. Numerical solutions in these two limits will be presented when only one of the terms in the step chemical potential corresponding to a particular form of step interaction is dominant at a time.

When only the quadratic term with G_2 is considered an initial sinusoidal surface decays exponentially in the DL regime as predicted by the continuum equations of motion in section 2 (equation (8)). However, in the SL regime the height of the corrugation decreases linearly with time. A similar behaviour of the height evolution of a corrugation has been predicted before in

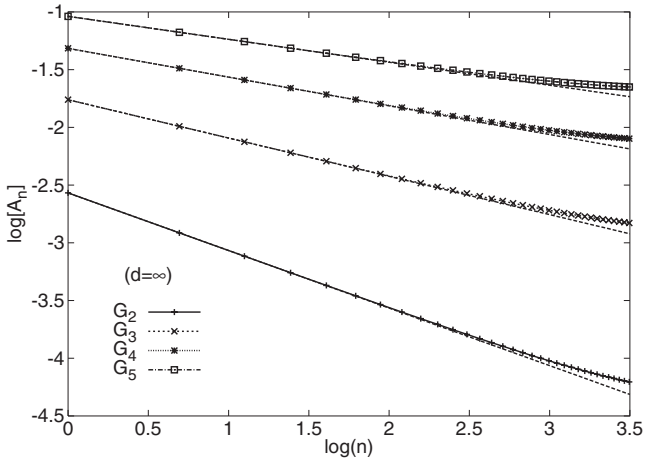

Figure 3. Similar to figure 2, but in the step attachment/detachment limited growth (SL) regime. The slopes corresponding to second-order (plus signs), third-order (crosses), fourth-order (filled circles with crosses) and fifth-order (open squares) interaction terms are $-1/2$, $-1/3$, $-1/4$ and $-1/5$, respectively.

connection with periodically modulated bidirectional crystal surfaces [16] and also during the decay of sinusoidal one-dimensional profiles below T_R where the anisotropic surface tension is replaced by an analytic yet sharply peaked function along the singular direction of the surface tension [17]. Figure 4 shows the time dependence of the height of the profile in the DL and SL regimes of surface processes when only the quadratic term in (2) is effective. As can be seen, the height decays exponentially for the DL regime and linearly in time in the SL regime until a small fraction of steps remain on the surface. The height evolution deviates from exponential and linear decay at the very late stages of the evolution as can be seen in figure 4. The symbols on the figures represent the times at which a step disappeared from the top (and bottom) of the profile. Whenever two steps are removed from the profile, the resulting surface no longer satisfies equation (37), but after a short transient time it quickly approaches that shape. As the number of steps remaining on the surface becomes a small fraction of the initial number of steps on the surface, the time dependence of the height of the corrugation begins to deviate from the expected behaviour. Furthermore, the height scales as λ^4 for the DL regime and as λ^3 for the SL regime where λ is the wavelength of the corrugation. But the shapes of the profiles are almost identical in the two cases as shown above with regard to solutions for the A_n. There is very little rearrangement of the initial surface for the present case since the initial profile is already a sine curve (see also figure 7). Note also that a nonlinear fit of the form $h(t) = a\exp(-bt^\eta)$ to the exponential decay gives $\eta = 1+\epsilon$ where $\epsilon \approx 0.05$ or less depending on the number of points considered in the fit. Since the decay deviates from the exponential behaviour when only a handful of steps remain on the surface, the data points corresponding to the late times of the height evolution are not considered in the fitting procedure. As the number of data points excluded from the fit corresponding to late times of evolution increases, the value of ϵ decreases but it never becomes exactly zero. A similar fit of the form $h(t) = a - bt^\eta$ for the linear decay gives similar results for the exponent η. The dashed lines on each curve in figure 4 represent the best least squares straight line fits to the corresponding data points on the curve. Each fit is made excluding the points relevant to late stages of evolution where only a few steps remain on the surface.

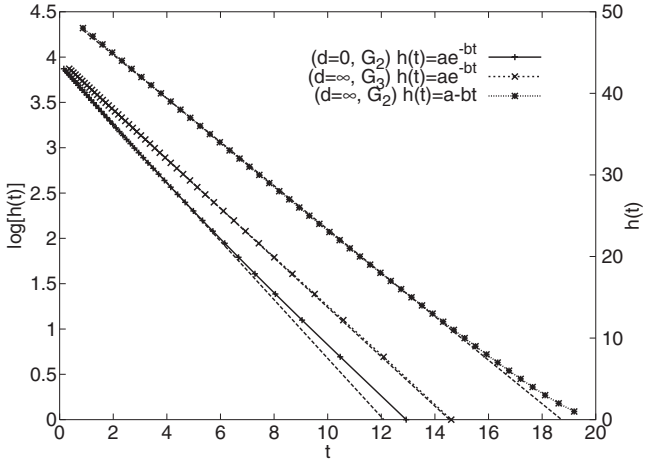

Figure 4. The time dependence of the height of the one-dimensional surface shown in figure 1 obtained from numerical solutions of equations (29) when only the quadratic term in equation (2) is effective in the DL regime (plus signs). A similar plot for the SL regime when the third-order term in equation (2) is effective (crosses) is also shown. The left-hand-side axis corresponds to these plots where a $\log[h(t)]-t$ curve is depicted. The right-hand-side axis (an $h(t)-t$ plot) is for the case where only the quadratic term in (2) is effective in the SL regime (filled circles with crosses) where the decay is linear with time. The dashed lines on each curve represent the best least squares straight line fits to the corresponding points. The fits are made excluding the data points related to very late stages of evolution where only a few steps remained on the surface. The symbols on the curves correspond to the time when a step disappeared from the top (and bottom) of the profile and both axes are in arbitrary units. The time axis is rescaled differently for the linear decay to fit the data into the graph appropriately.

Next we treat the case where only the third-order term with G_3 is considered in the surface free energy. Since this case is studied in detail in [3] we will just mention that the surface profile decays inversely in time in the DL regime and exponentially in time in the SL regime as correctly pointed out by [18], clarifying a confusion that arose in [3]. Figure 4 depicts the variation of the height of the surface in the SL regime when the third-order term in equation (2) is effective. As one can see from the figure, the height decays exponentially until only a few steps remain on the surface. The variation of the height for the DL regime is shown in figure 5 and as can be seen decays inversely with time. The scaling of the height goes in this case as λ^4 for the SL regime and as λ^5 for the DL regime with respect to the wavelength of the corrugation. The shapes of the profiles for the DL and SL regimes for this case are also almost identical. A nonlinear fit of the form $h(t) = a\exp(-bt^{\eta})$ for the SL regime and of the form $[h(t)]^{-1} = a - bt^{\eta}$ for the DL regime give similar results for η to that in the case where only the quadratic interaction term is considered, above.

The solution of equations (29) when only the fourth-order term is present in the surface free energy in (2) shows that the height of the corrugation decays as $t^{-1/2}$ in the DL regime and as t^{-1} in the SL regime. The $t^{-1/2}$ dependence was also predicted by the continuum equations (equation (18)). The time dependence of the height of the corrugation is shown in figure 5 for the DL and SL cases. The scalings of the height for the DL and SL cases are λ^6 and λ^5, respectively. Finally, when only the fifth-order term in the expansion for the surface free energy is considered, the height of the surface decays as $t^{-1/3}$ in the DL regime and as $t^{-1/2}$ in the SL regime. Again the DL regime solution for the height is identical to the form predicted by the continuum equations. The height evolution for the SL regime is shown in figure 5 and

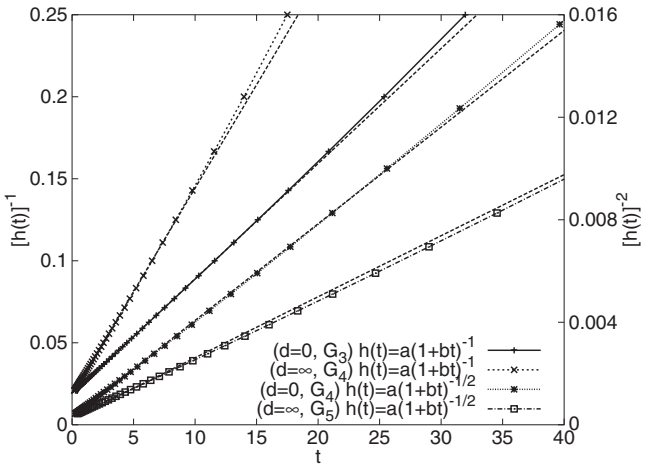

Figure 5. Similar to figure 4, but when only the third-, fourth- and fifth-order terms in equation (2) are effective in various dominant surface processes. The left-hand-side axis relates to the curves with crosses and plus signs and the right-hand-side axis relates to the curves with filled circles with crosses and open squares. The height decays inversely with time in the DL regime when the third-order term in (2) is dominant (plus signs) and also in the SL regime when the fourth-order term in (2) is dominant (crosses). The height of the crystal decreases inversely with the square root of time in the DL regime when the fourth-order term in (2) is dominant (filled circles with crosses) and the same time dependence occurs in the SL regime when the fifth-order term is dominant (open squares). The left-hand-side axis corresponds to $[h(t)]^{-1}-t$ plots and the right-hand-side axis is for an $[h(t)]^{-2}-t$ plot. The dashed lines on each curve represent the best least squares straight line fits to the corresponding points. The fits are made excluding the data points related to very late stages of evolution where only a few steps remained on the surface. The symbols on the curves correspond to the time when a step disappeared from the top (and bottom) of the profile and both axes are in arbitrary units. The time axis is rescaled differently for the left-hand-side and right-hand-side axes to fit the data into the graph appropriately.

that for the DL regime in figure 6. The scaling of the height for the present case turns out to be λ^7 for the DL case and λ^6 for the SL case. For the present cases a nonlinear fit of the form $[h(t)]^{-n} = a - bt^{\eta}$ where n is the appropriate exponent for the relevant interaction and surface process gives again values for η similar to those in the previous cases considered above.

There are common points for all cases considered above: the surface rearranges itself considerably at the beginning (except for in the case of quadratic interactions) for a certain period of time until it reaches the shape preserving solution predicted by equation (37) appropriate for the dominant step–step interaction. The ledges close to the top (and bottom) of the profile approach this shape faster than the others because they can release/capture particles much more easily so they have a greater ability to move. While the form of step interaction determines the shape of the evolving profile, the dominant surface process (DL or SL) determines the evolution of terrace widths, which in turn determine the evolution of the height of the corrugation. Whenever two steps disappear from the profile (from the top and bottom by symmetry) the resulting surface profile does not strictly follow the form given in (37) but after a short transient time approaches this shape. The continuum equations and discrete equations give identical results for the evolution of the height of the crystal in the diffusion limited growth regime. Scaling of the height with wavelength takes place for all cases. These results are summarized in table 1.

To complete the treatment of the subject we show the time dependence of the terrace widths and compare the numerical results with those from analytical solutions given in (32) and (33).

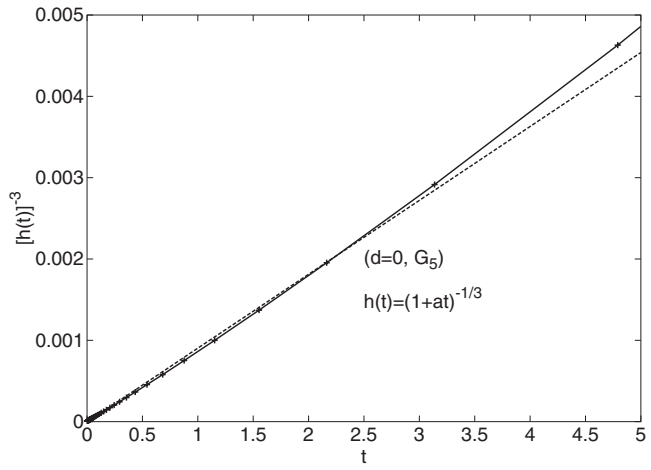

Figure 6. Similar to figure 4, but when only the fifth-order term in equation (2) is effective in the DL regime (plus signs) and the best straight line fit to this curve (dashed line). The surface height decays inversely with the third root of time as seen in the figure. Both axes are in arbitrary units.

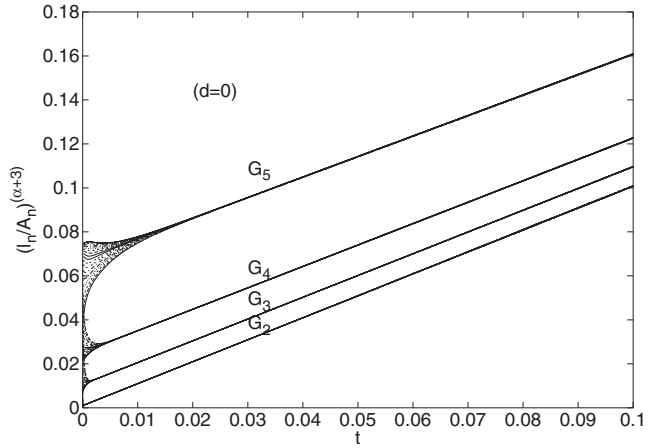

Figure 7. The time variation of the ratio $(\ell_n(t)/A_n)^{(\alpha+3)}$ in the DL regime when there are 20 steps on the surface. The $\ell_n(t)$ are found from the numerical solution of equation (30) and the A_n are found from numerical solution of equations (34), (35). $\alpha = 1, 2, 3$ or 4 when second-order (G_2), third-order (G_3), fourth-order (G_4) and fifth-order (G_5) terms in (2) are dominant, respectively. The initial surface is a sine curve and the top (and bottom) of the profile for this case is only chosen so long that the profile reaches the shape preserving solution appropriate for the type of step interaction under consideration without any step collisions and annihilations. As one can see from the figure, terrace separations vary until the shape preserving solution (37) is reached at which all ratios converge to a single value for each value of α. The labels on each curve indicate the dominant step–step interaction term. Both the horizontal and vertical axes are normalized to unity; therefore the values along the vertical axis are not proportional for each curve. Note that while there is almost no rearrangement of the profile for quadratic interactions, there is considerable rearrangement for the other interaction terms in equation (2).

The quantity $(\ell_n(t)/A_n)^{(\alpha+3)}$ is plotted as a function of time in figure 7; when there are a total of 40 terraces on the initial surface, the first 20 of them are shown in the figure. Since our aim is to test the proposed analytical solutions which are valid only after the surface profile assumes the

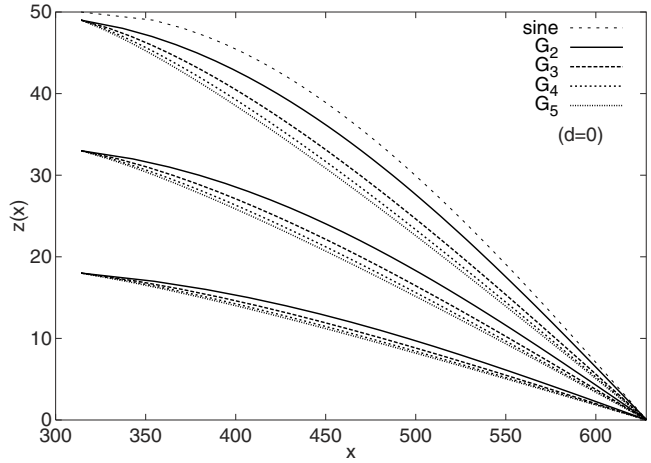

Figure 8. Comparison of the surface profiles obtained by the numerical solution of equation (29) when only the second-order (straight curves), third-order (heavy dashed curves), fourth-order (short dashed curves) and fifth-order (dots) terms in (2) are dominant at a time at various equal crystal heights. The profiles shown at a particular height correspond to a time when a step from the top (and bottom) of the surface is just about to disappear. The initial surface is a sine curve (dashed curve).

shape preserving solution (37), for these plots only the top and bottom of the profile is chosen very long to prevent step annihilation at the top (and step coalescence at the bottom) so that the surface approaches the shape preserving solution (37) after a while. The values corresponding to vertical and horizontal axes are first normalized to unity and then plotted. Therefore the values on the vertical axis are not proportional. Both axes in the figure are in arbitrary units. As can be seen in the figure, while surface rearrangement occurs for third-, fourth- and fifth-order interactions in (2), it is almost nonexistent for the case of quadratic interactions. This shows that an initial sine curve is already almost the shape preserving solution for the quadratic interactions. This was also the case for continuum equations as shown in section 2.

The appearances of surface profiles at different times for different step interactions are shown in figure 8 at equal surface heights. The profiles shown are at a time when a step from the top is just about to disappear and the curves are obtained by passing straight lines through step positions. It is expected that the top of the profile must obey $\delta z = (x - x_0)^{(\alpha+1)/\alpha}$ where x_0 is the edge of the top facet and $\alpha = 1, 2, 3$ or 4. We made no attempt to find the exponent for the top of the profile because it is observed that the exponent sensitively depends on the value of x_0 chosen.

4. Conclusions

In this paper the evolution of the height of a crystal surface and its shape as functions of time are investigated when one form of step–step interactions is dominant at a time. Only surface diffusion is considered as a means of mass transfer. Continuum equations for surface evolution and discrete equations of motion for individual steps in the diffusion limited growth regime lead to the same form of variation of the height of the crystal. Additional time dependences of terrace widths and thus the height of the crystal result in step attachment/detachment limited growth for the case of discrete equations for steps. The height of the crystal decays as a function of time as e^{-t} or t^c where $c = 1, -1, -1/2$ or $-1/3$ depending on the dominant

type of step–step interaction and surface process. Furthermore, it is found that the height of the crystal scales with the wavelength of the corrugation for all types of step–step interaction and rate limiting surface process considered. While step interactions determine the shape of the evolving surface, the dominant surface process controls the time dependence of the terrace widths and thus of the height of the crystal for a given type of step interaction potential. Therefore both the shape of the surface and the variation of its height as a function of time should be known to determine both the dominant type of step–step interaction and the growth limiting surface process. These results may be used in interpreting experimental results.

References

[1] For a review see
Giesen M 2001 *Prog. Surf. Sci.* **68** 1
Jeong H C and Williams E D 1999 *Surf. Sci. Rep.* **34** 171
Ogino T, Hibio H and Homma Y 1999 *Crit. Rev. Solid State Mater. Sci.* **24** 227

[2] van Beijeren H and Nolden I 1987 *The Roughening Transition, Structure and Dynamics of Surfaces II* (*Springer Topics in Current Physics* vol 43) ed W Schommers and P von Blanckenhagen (Berlin: Springer) p 259

[3] Ozdemir M and Zangwill A 1990 *Phys. Rev.* B **42** 5013

[4] Andreev A F and Kosevich Yu A 1981 *Zh. Eksp. Teor. Fiz.* **81** 1435
Andreev A F and Kosevich Yu A 1981 *Sov. Phys.—JETP* **54** 761 (Engl. Transl.)

[5] Pearson E M, Halicioglu T and Tiller W A 1987 *Surf. Sci.* **184** 401

[6] Andreev A F 1981 *Zh. Eksp. Teor. Fiz.* **81** 2042
Andreev A F 1981 *Sov. Phys.—JETP* **53** 1063 (Engl. Transl.)

[7] Gruber E E and Mullins W W 1967 *J. Chem. Solids* **28** 875

[8] Saenz J J and Garcia N 1985 *Surf. Sci.* **155** 24

[9] Garcia N and Serena P A 1995 *Surf. Sci.* **330** L665

[10] Jayaprakash C and Saam W F 1984 *Phys. Rev.* B **30** 3916

[11] Najafabadi R and Sorolovitz D 1994 *Surf. Sci.* **317** 221

[12] Herring C 1951 *The Physics of Powder Metallurgy* ed W E Kingston (New York: McGraw-Hill) p 143

[13] Mullins W W 1959 *J. Appl. Phys.* **30** 77

[14] Mullins W W 1963 *Metal Surfaces* ed W D Robertson and N A Gjostein (Metal Park, OH: American Society for Metals) p 17

[15] Lançon F and Villain J 1990 *Kinetics of Ordering and Growth at Surfaces* ed M Lagally (New York: Plenum)

[16] Rettori A and Villain J 1988 *J. Physique* **49** 257

[17] Bonzel H P and Preuss E 1995 *Surf. Sci.* **336** 209

[18] Israeli N and Kandel D 2002 *Phys. Rev. Lett.* **88** 169601

[19] Press W H, Flannery B P, Teukolsky S A and Vetterling W T 1986 *Numerical Recipes: the Art of Scientific Computing* (Cambridge: Cambridge University Press)